

Virtual Receiver Matrix for Multifunction Communication and Sensing Wireless Systems Using Simultaneous Incident Waves at the Same Carrier Frequency

Seyed Ali Keivaan, Pascal Burasa, Ke Wu

Poly-Grames Research Center, Polytechnique Montréal, Canada

{seyed-ali.keivaan, pascal.burasa, ke.wu}@polymtl.ca

Abstract— In this paper, simultaneous reception and demodulation of incident signals at the same carrier frequency is proposed and demonstrated. Not only this technique significantly enhances the communication capacity, but also most importantly, it enables multifunction communication and sensing applications. This technique is set to exploit both the phase difference and the angle-of-arrival (AoA) of incoming waves to demodulate multiple and simultaneous incident signals at the same carrier frequency. In addition, this is made possible through the combinatory and dynamic allocation of activated receiving units that are spatially distributed in the virtual receiver matrix (VRM). The theoretical analysis is studied in this work and as a proof-of-concept, a prototype is fabricated for 5G applications. The measurement results show EVM of less than 10% for the two distinct QPSK signals.

Keywords— Interferometric techniques, multiport receiver, millimeter-wave, terahertz (THz), spatially distributed receiver, virtual receiver matrix, 5G, 6G and future multifunction wireless.

I. INTRODUCTION

Over the last decades, five generations of wireless technology have been introduced and deployed, with each enabling features and services, providing breakthrough enhancements in terms of communication capacity and quality. Generally, they take advantage of networks with multiple base stations and access points [1]. However, future multifunction wireless communication and sensing systems under the umbrella of 6G and beyond [2], should substantially upgrade their standards to keep pace with the insatiable demand for ever-increasing intelligence, capacity and low latency driven by a projected rising number of smart terminals and data traffics [3]. In this connection, disruptive and innovative solutions are required to redefine the architectures of existing wireless systems [4]. Recently, a new receiver topology, named virtual receiver matrix (VRM), has been introduced [5], which accommodates multifunctionality in a smart, dense, and efficient manner, while it tremendously increases the number of potential receivers or receiving channels in a dynamic configuration compared to conventional fixed receivers.

In this paper, data reception and demodulation of two simultaneous incoming signals having the same carrier frequency is proposed and demonstrated with the VRM concept, thereby greatly enhancing communication capacity and multifunctionality. In fact, data reception for multiple incident signals is enabled by the VRM concept, consisting of a dynamic allocation of activated receiving units, spatially

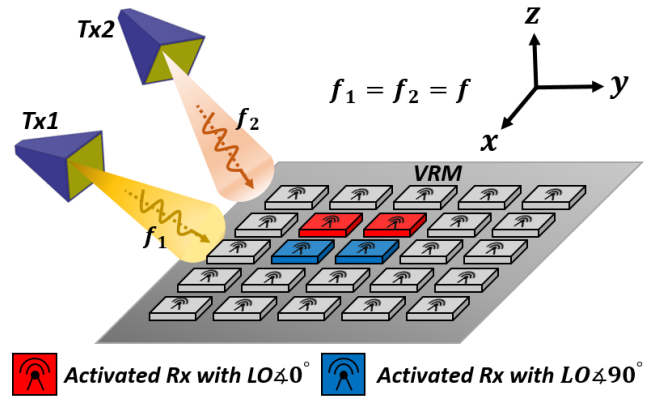


Fig. 1. Conceptual illustration of VRM demodulating two incident signals at the same carrier frequencies, simultaneously. Two red activated units extract quadrature components while the two blue ones demodulate in-phase components of the two incident signals.

distributed in a two-dimensional (2D) matrix. By using the phase difference of incident waves with diversified AoAs, we can demodulate multiple and simultaneous incident signals at the same carrier frequency.

In the following, the theoretical background for demodulating two incident signals is studied and discussed. As a proof-of-concept, an experimental prototype is fabricated and measured at Ka-band for 5G multifunction applications, which is set to receive two distinct sources at the same carrier frequency. In the fabricated prototype, each unit-cell demodulates either in-phase or quadrature components of an incoming QAM signal. The measurement results confirm the data receiving operation for both simultaneous incident signals.

II. THEORETICAL ANALYSIS

The proposed VRM unit-cells, illustrated in Fig. 2, involve a RF antenna, a low noise amplifier (LNA), a 90-degree hybrid coupler, and two power detectors connected in a differential and balanced form. Other forms of unit-cells are also possible. The local oscillator (LO) signal is injected into each unit-cell through the other port of the hybrid coupler. To avoid the leakage of LO into the antenna, these two ports should be designed with maximum possible isolation. In the following, the theoretical analysis of data reception for two different incoming signals having the same carrier frequency

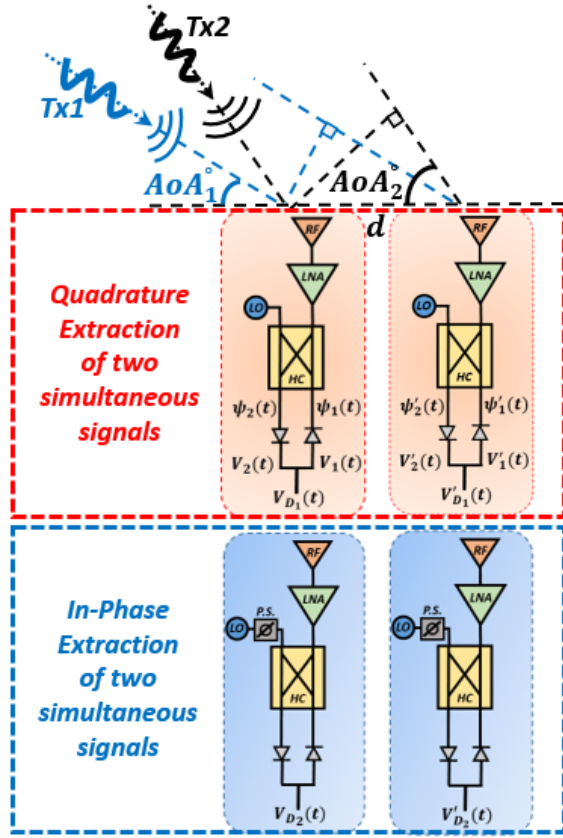


Fig. 2. Block diagram of 2D VRM unit-cells, each containing an antenna, a LNA, a 90-degree hybrid coupler, and two power detectors connected in a differential and balanced form. Two different signals at the same carrier frequency are incident on the VRM unit-cells with different AoAs, simultaneously. (P.S. and HC are short for phase shifter and hybrid coupler, respectively).

is presented. In the case of a coherent receiver, the frequency of carrier at both transmitter and receiver is considered the same for both transmitted signals. Considering the proposed configuration for each unit-cell of VRM in Fig. 2, the received signal after the LNA of the first unit-cell is

$$S_{RF}(t) = a_{RF}\alpha_1(t)e^{j(\omega t + \theta_1(t))} + a_{RF}\alpha_2(t)e^{j(\omega t + \theta_2(t))} \quad (1)$$

where $\alpha_1(t), \alpha_2(t)$ and $\theta_1(t), \theta_2(t)$ are the modulated amplitude and phase of transmitted baseband signals, respectively. If we also consider the injected LO signal as

$$S_{LO}(t) = a_{LO}e^{j\omega t} \quad (2)$$

then, the output signals of the 90-degree hybrid coupler ports can be obtained as

$$\psi_1(t) = \frac{-a_{LO}}{\sqrt{2}}e^{j\omega t} \left[j \frac{a_{RF}}{a_{LO}}\alpha_1(t)e^{j\theta_1(t)} + j \frac{a_{RF}}{a_{LO}}\alpha_2(t)e^{j\theta_2(t)} + 1 \right] \quad (3)$$

$$\psi_2(t) = \frac{-a_{LO}}{\sqrt{2}}e^{j\omega t} \left[\frac{a_{RF}}{a_{LO}}\alpha_1(t)e^{j\theta_1(t)} + \frac{a_{RF}}{a_{LO}}\alpha_2(t)e^{j\theta_2(t)} + j \right] \quad (4)$$

These two signals are connected to power detectors with opposite polarities, thus resulting in baseband signals proportional to their input RF power

$$V_i(t) = K|\psi_i(t)|^2, i = 1, 2 \quad (5)$$

where K is a constant determined by the type of power detectors. Accordingly, the output voltages of power detectors are described as follows

$$V_1(t) = \frac{K a_{LO}^2}{2} \left[1 + \left(\frac{a_{RF}}{a_{LO}} \right)^2 \alpha_1^2(t) + \left(\frac{a_{RF}}{a_{LO}} \right)^2 \alpha_2^2(t) - 2 \frac{a_{RF}}{a_{LO}} \alpha_1(t) \sin(\theta_1(t)) - 2 \frac{a_{RF}}{a_{LO}} \alpha_2(t) \sin(\theta_2(t)) \right] \quad (6)$$

$$V_2(t) = \frac{K a_{LO}^2}{2} \left[1 + \left(\frac{a_{RF}}{a_{LO}} \right)^2 \alpha_1^2(t) + \left(\frac{a_{RF}}{a_{LO}} \right)^2 \alpha_2^2(t) + 2 \frac{a_{RF}}{a_{LO}} \alpha_1(t) \sin(\theta_1(t)) + 2 \frac{a_{RF}}{a_{LO}} \alpha_2(t) \sin(\theta_2(t)) \right] \quad (7)$$

Since the power detectors are configured in a differential form, their differential output voltage becomes

$$V_{D1}(t) = 2K a_{LO} a_{RF} [\alpha_1(t) \sin(\theta_1(t)) + \alpha_2(t) \sin(\theta_2(t))] \quad (8)$$

The phase differences between received signals at two distinct antennas in different cells can be formulated as follows,

$$\Delta\phi_1 = \frac{2\pi d}{\lambda} \cos(AoA_1), \quad \Delta\phi_2 = \frac{2\pi d}{\lambda} \cos(AoA_2) \quad (9)$$

where d is the inter-element distance between any two cells distributed in the matrix, λ is the operational wavelength, and AoA_1 and AoA_2 are the angle of arrivals of the two incident waves. By considering these two phase differences, we can obtain the RF signal after the LNA of the second unit-cell as

$$S'_{RF}(t) = a_{RF}\alpha_1(t)e^{j(\omega t + \theta_1(t))} \cdot e^{-j\Delta\phi_1} + a_{RF}\alpha_2(t)e^{j(\omega t + \theta_2(t))} \cdot e^{-j\Delta\phi_2} \quad (10)$$

Again, after injecting LO power to the hybrid coupler of the second unit-cell, the signals before the power detectors can be obtained as

$$\psi'_1(t) = \frac{-a_{LO}}{\sqrt{2}}e^{j\omega t} \left[j \frac{a_{RF}}{a_{LO}}\alpha_1(t)e^{j(\theta_1(t) + \Delta\phi_1)} + j \frac{a_{RF}}{a_{LO}}\alpha_2(t)e^{j(\theta_2(t) + \Delta\phi_2)} + 1 \right] \quad (11)$$

$$\psi'_2(t) = \frac{-a_{LO}}{\sqrt{2}}e^{j\omega t} \left[\frac{a_{RF}}{a_{LO}}\alpha_1(t)e^{j(\theta_1(t) + \Delta\phi_1)} + \frac{a_{RF}}{a_{LO}}\alpha_2(t)e^{j(\theta_2(t) + \Delta\phi_2)} + j \right] \quad (12)$$

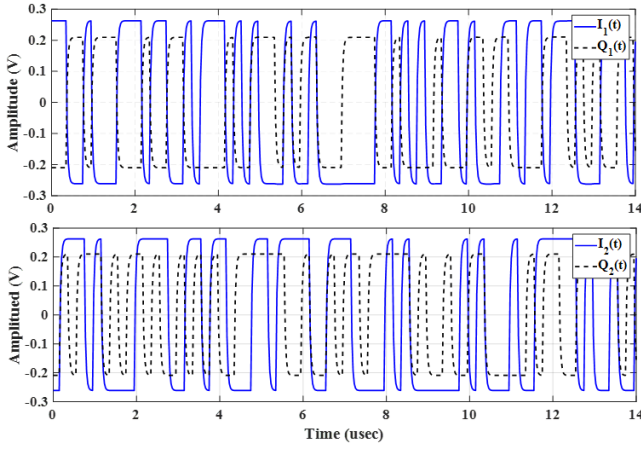


Fig. 3. Simulated in-phase and quadrature components of two simultaneous incident signals at the same carrier frequency for QPSK modulation with data rate of 2 MSPs.

Therefore, the output voltages of power detectors can be calculated as

$$V'_1(t) = \frac{K a_{LO}^2}{2} \left[1 + \left(\frac{a_{RF}}{a_{LO}} \right)^2 \alpha_1^2(t) + \left(\frac{a_{RF}}{a_{LO}} \right)^2 \alpha_2^2(t) - 2 \frac{a_{RF}}{a_{LO}} \alpha_1(t) \sin(\theta_1(t) + \Delta\phi_1) - 2 \frac{a_{RF}}{a_{LO}} \alpha_2(t) \sin(\theta_2(t) + \Delta\phi_2) \right] \quad (13)$$

$$V'_2(t) = \frac{K a_{LO}^2}{2} \left[1 + \left(\frac{a_{RF}}{a_{LO}} \right)^2 \alpha_1^2(t) + \left(\frac{a_{RF}}{a_{LO}} \right)^2 \alpha_2^2(t) + 2 \frac{a_{RF}}{a_{LO}} \alpha_1(t) \sin(\theta_1(t) + \Delta\phi_1) + 2 \frac{a_{RF}}{a_{LO}} \alpha_2(t) \sin(\theta_2(t) + \Delta\phi_2) \right] \quad (14)$$

The differential output of the second unit-cell can be written as

$$V'_{D_1}(t) = 2K a_{LO} a_{RF} [\alpha_1(t) \sin(\theta_1(t) + \Delta\phi_1) + \alpha_2(t) \sin(\theta_2(t) + \Delta\phi_2)] \quad (15)$$

Therefore, by setting $\Delta\phi_1 = 2n\pi$ and $\Delta\phi_2 = 2n\pi + \pi$, we can readily find the quadrature components of the two signals

$$Q_1(t) = V_{D_1}(t) + V'_{D_1}(t) \quad \& \quad Q_2(t) = V_{D_1}(t) - V'_{D_1}(t) \quad (16)$$

Until now, we have obtained the quadrature components of the two incident signals with the same carrier frequency. For the in-phase components, another set of two unit-cells should be chosen with this difference that their injected LO should have a 90-degree phase shift. Using a similar procedure from (1) to (16) we can establish the following formulas for their differential output voltages.

$$V_{D_2}(t) = 2K a_{LO} a_{RF} [\alpha_1(t) \cos(\theta_1(t)) + \alpha_2(t) \cos(\theta_2(t))] \quad (17)$$

$$V'_{D_2}(t) = 2K a_{LO} a_{RF} [\alpha_1(t) \cos(\theta_1(t) + \Delta\phi_1) + \alpha_2(t) \cos(\theta_2(t) + \Delta\phi_2)] \quad (18)$$

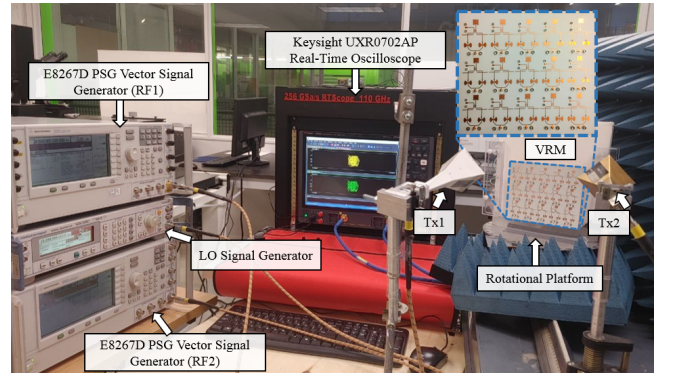


Fig. 4. Photograph of the measurement setup for demodulating two simultaneous incident signals with different AoAs over the VRM.

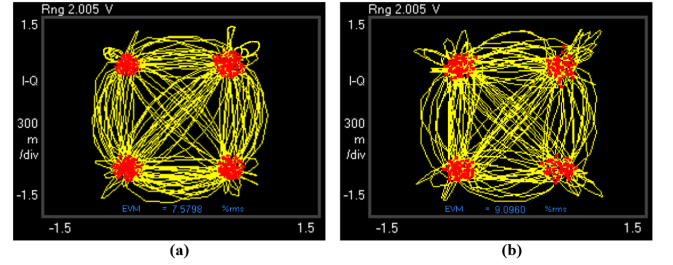


Fig. 5. Measured constellations of two simultaneous incident signals with different AoAs.

Hence, by setting the same conditions for phase differences we can readily find out the in-phase components of the two signals

$$I_1(t) = V_{D_2}(t) + V'_{D_2}(t) \quad \& \quad I_2(t) = V_{D_2}(t) - V'_{D_2}(t) \quad (19)$$

Now, considering complex vectors of $S_1(t) = I_1(t) + jQ_1(t)$, and $S_2(t) = I_2(t) + jQ_2(t)$, the two demodulated signals can be extracted, separately. The simulation results of extracted in-phase and quadrature components of the proposed configuration of VRM unit-cells in Keysight Advanced Design System (ADS) software is shown in Fig.3 for a data rate of 2MSPs.

III. DESIGN METHODOLOGY AND PERFORMANCE ANALYSIS

For the proof-of-concept, a VRM prototype of 3x5 unit-cells is designed and fabricated on Rogers RO4350 over Ka-band for 5G applications. This is to receive two signals at the same carrier frequency, simultaneously, as shown in Fig. 4. The prototype is designed and analyzed in ADS software platform and full-wave simulations are performed in CST software to design the antenna and hybrid couplers. The output voltages of power detectors (SMS7630-040LF) are connected to Keysight UXR0702AP Real-Time Oscilloscope to demonstrate the constellations of demodulated signals. Through the use of Agilent PSG vector signal generator E8267D, a bit train of QPSK modulation scheme with a symbol rate of 2 Msp/s is generated. All the generators and

analyzers are synchronized to ensure the coherency of receiver. The VRM is placed on a rotational platform to adjust the desired AoAs with respect to the horn radiators. Considering the designed unit-cells with the inter-element distance of two wavelengths, the AoAs should be 60.0 and 75.5 degrees. Fig. 5 shows the measured constellation diagrams of the VRM prototype for the two incident signals, to validate the receiving operation. The receiver EVM is less than 10% for both signals.

IV. CONCLUSION

This work proposed and presented the demodulation of simultaneous incident signals featuring the same carrier frequency, for the first time. This seamless architecture technique, which is made possible through the concept of VRM, greatly enhances the capacity and multifunctionality of future wireless systems. A mathematical modeling of the proposed technique was derived and presented. As a proof-of-concept, a fabricated prototype was measured at Ka-band for 5G applications, and measurements results have confirmed the viability of the proposed technique.

REFERENCES

- [1] C. Wang et al., "Cellular architecture and key technologies for 5G wireless communication networks," *IEEE Communications Magazine*, vol. 52, no. 2, pp. 122-130, February 2014.
- [2] N. Chi, Y. Zhou, Y. Wei and F. Hu, "Visible Light Communication in 6G: Advances, Challenges, and Prospects," *IEEE Vehicular Technology Magazine*, vol. 15, no. 4, pp. 93-102, Dec. 2020.
- [3] K. Chuang, H. Yektaei, D. McLaurin and C. Mayer, "Radio Challenges, Architectures, and Design Considerations for Wireless Infrastructure: Creating the Core Technologies That Connect People Around the World," in *IEEE Microwave Magazine*, vol. 23, no. 12, pp. 42-59, Dec. 2022.
- [4] J. Moghaddasi and K. Wu, "Multifunction, Multiband, and Multimode Wireless Receivers: A Path Toward the Future," *IEEE Microwave Magazine*, vol. 21, no. 12, pp. 104-125, Dec. 2020.
- [5] S.A. Keivaan, P. Burasa. and K. Wu, "Virtual Receiver Matrix and Combinatory Analog Operations for Future Multifunction Reconfigurable Sensing and Communication Wireless Systems", in *IEEE Transactions on Microwave Theory and Technique*, Dec 2022.